Coverage Prediction with UTD Model

Alp Eren Aydin, Mehmet Baris Tabakcioglu
Electrical and Electronics Engineering
Bursa Technical University, Bursa, Turkey

Eray Arik
EMC Division
Ermaksan, Bursa, Turkey

***Abstract*— Coverage prediction is vital for reliable communication systems. In order to increase QoS, threshold field strength have to be ensured and coverage map extracted. Uniform Theory of diffraction (UTD) model is used to calculate electric field. In this study, a scenario including 441 buildings is generated randomly and electric field is calculated at the top of all buildings. According to electric field coverage map is extracted.**

Keywords—Coverage mapping; UTD; diffraction; wave propagation

I. Introduction

Coverage prediction is significant to install reliable and efficient wireless communication systems. Base stations have to be deployed after coverage prediction done. In order to calculate electric field, Geometrical Optic (GO) and Uniform theory of diffraction (UTD) model [1] is used. In order to increase the QoS of wireless communication systems, firstly coverage prediction is carried out. Geometrical optic model assumes that light propagates as a particle and explains reflection and refraction phenomena. However GO model cannot explain diffraction phenomena [2]. UTD model is introduced in order to solve problem of electric field behind an obstacle. UTD is a high frequency model and computes the electric field in a short time. In order to reduce base station number and increase QoS of broadcasting systems, coverage map have to be extracted. Coverage mapping can be made by means of some radio planning tools like FEKO [3] and ACCURA [4]. Ray-tracing is important to obtain more accurate coverage maps [5-7]. In the rest of paper, brief information about UTD is given, then a coverage prediction simulation is carried out and conclusion section is given.

II. UTD Model

Electric field behind an obstacle in UTD model can be found by the formula [8] given by,

$$E = [E_i D] A(s) e^{-jks} \tag{1}$$

where, E_i and D are incident field and amplitude diffraction coefficient, k stands for wave number, *A(s)* symbolize spreading factor and finally s is travelling distance of electromagnetic wave. The amplitude diffraction coefficient [9] is expressed by,

$$D(\alpha) = -\frac{e^{-j\pi/4}}{2\sqrt{2\pi k}\cos(\alpha/2)} F[x] \tag{2}$$

where,
α is diffraction angle as illustrated in Fig. 1. $F[x]$ is transition function in [10] and changes between 0 and 1.

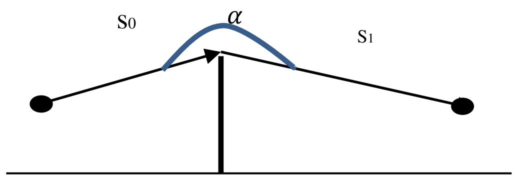

Fig.1. Diffraction Geometry

A(s) is spreading factor and can be calculated by,

$$A(s) = \sqrt{\frac{s_0}{s_1(s_1+s_0)}} \tag{3}$$

where, s_0 and s_1 are the distance before and after the diffraction, respectively. Reflected field can be expressed by,

$$E = \left[\frac{E_i R_{s,h}}{s}\right] e^{-jks} \tag{4}$$

where, E_i is incident field, s is total distance and $R_{s,h}$ is reflection coefficient for soft and hard polarizations. Direct field can be calculated by

$$E = \left[\frac{E_i}{s}\right] e^{-jks} \tag{5}$$

where, E_i is incident field and s is total distance.

III. Coverage Prediction

In order to calculate total electric field in a point, diffracted, reflected and direct fields have to be calculated via the formulas previously mentioned. An extensive simulation is carried out with 1800 MHz operating frequency. A building matrix (21x21) is generated with height of buildings in z-direction. This matrix includes randomly distributed 441 building's heights between 0 and 20 as shown in Table I. 21 buildings are deployed uniformly x and y direction between 0-1000. In this study firstly, transmitter and receiver location is selected (0,0) and (0,1000), respectively as depicted in Fig.2.

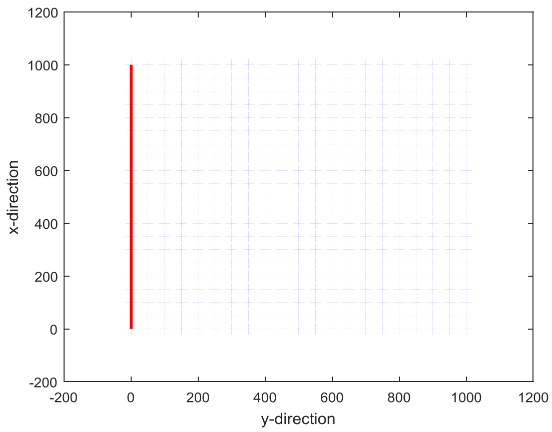

Fig. 2. Buildings are in x-direction

As it is illustrated in Fig.2, all the buildings are in x-direction. These buildings are shown in test scenario as in Fig. 3.

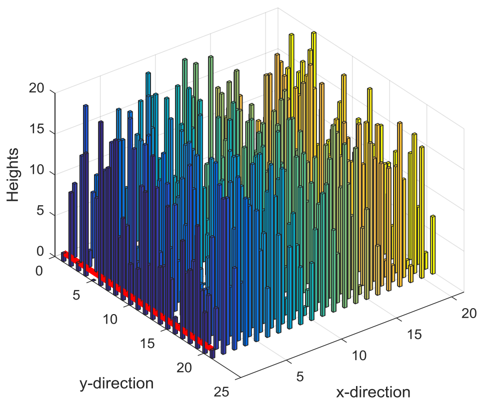

Fig. 3. Buildings in test scenario

As it is shown in Fig. 3, buildings in x-direction are shown with red line. All the rays emanate from the transmitter and reach to receiver are indicated in Fig. 4.

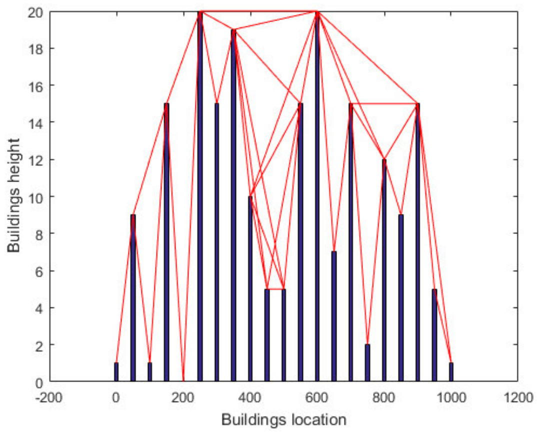

Fig. 4. Ray tracing

As shown in Fig. 4, all the ray paths contributing to total electric field at the receiving point are given. Secondly, transmitter and receiver location is selected (0,0) and (1000,1000), respectively as depicted in Fig.5.

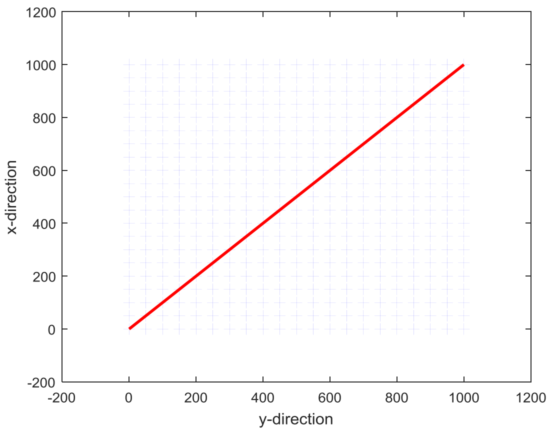

Fig. 5. Buildings are in xy-direction

As it is illustrated in Fig. 5, the buildings are deployed in xy-direction. These buildings are shown in test scenario as in Fig. 6.

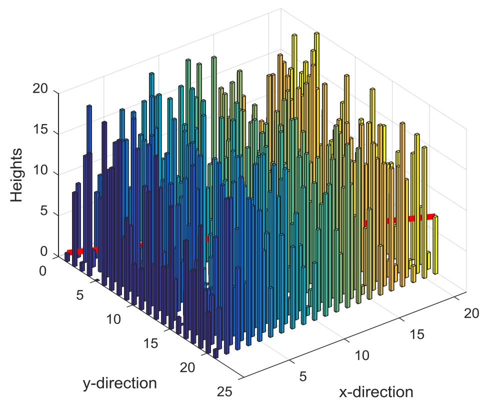

Fig. 6. Buildings in test scenario

As it is shown in Fig. 6, buildings in xy-direction are shown with red line. All the rays emanate from the transmitter and reach to receiver are indicated in Fig. 7.

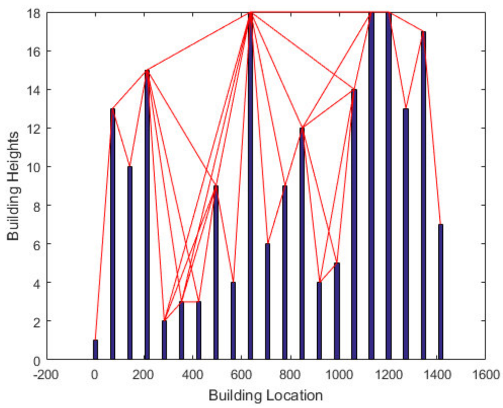

Fig. 7. Ray tracing

As shown in Fig. 7, all the ray paths contributing to total electric field at the receiving point are given. Receiver position is changed one by one and electric fields are calculated all the positions. The electric fields in all receiving positions are given in Table II. As can be seen in Table II, as the transmitter is in (0,0) position, value of electric field is assumed to 1 and dB value of the electric field is zero. Moreover, it can be seen in Table II, as the receiving point is farther away, electric field is decreases. Furthermore, if there is multiple diffraction (x-direction, y-direction and diagonal), electric field is decreased greatly as it is shown in Table II.

IV. Conclusions

Predicting of electric field is very important to install reliable and efficient broadcasting systems in radio planning tool. After predicting the field strength, base stations have to be deployed according to results. In multiple diffraction scenarios UTD and Geometrical optic models have to be used together. If the receiver is away from the transmitter, electric field decreases. As the receiving point move in x, y or diagonal, electric fields decreases greatly. As a conclusion, in order to increase QoS in broadcasting system or reducing base station number coverage mapping have to be made firstly.

Acknowledgment

This work is supported partially by TÜBİTAK (The Scientific and Technological Research Council of Turkey) under the grant no. 215E360.

References

[1] R.G. Kouyoumjian and P.H. Pathak, “Uniform geometrical theory of diffraction for an edge in a perfectly conducting surface”, Proceedings of IEEE, vol. 62, no: 11, pp.1448–1461, 1974.

[2] V.A. Borovikov and B.E. Kinber, “Geometrical Theory of Diffraction”, Institution of Electrical Engineers, London, UK, 1994.

[3] https://www.feko.info

[4] http://www.wavecall.com

[5] E. Arik and M.B. Tabakcioglu, “Using of S-UTD-CH model in coverage mapping and comparison with FEKO software”, 25th Signal Processing and Communications Applications Conference, pp. 1-4, 2017.

[6] M.B. Tabakcioglu, “A Top-down Approach to S-UTD-CH Model”, ACES Journal, vol. 32, no:7, pp.586-592, 2017.

[7] M.B. Tabakcioglu, “S-UTD-CH model in multiple diffractions”, International Journal of Electronics, vol. 103, no:5, pp. 765-774, 2017.

[8] R. J. Luebbers, “A General, Uniform Double Wedge Diffraction Coefficient”, IEEE Transactions on Antennas and Propagation, vol. 39. no. 1, pp. 8–14, 1989.

[9] C. Tzaras, S. and R. Saunders, “An improved heuristic UTD solution for multiple- edge transition zone diffraction,” IEEE Transactions on Antennas Propagatios, vol. 49, no. 12, 2001.

[10] D. A. McNamara, C. V. Pistorious, J. A. G. Malherbe, “Introduction to the Uniform Geometrical Theory of Diffraction”, Boston. MA: Artech House, 1990.

TABLE I. Height of Building

1	9	1	15	0	20	15	19	10	5	5	15	20	7	15	2	12	9	15	5	1
9	13	2	9	13	17	6	8	18	14	5	15	6	5	0	7	9	6	6	5	19
18	8	10	11	10	5	20	3	18	0	6	15	13	3	19	11	5	12	19	18	10
9	6	1	15	2	7	8	18	0	17	6	5	10	15	4	4	20	12	6	20	18
3	0	14	18	2	0	12	12	10	0	14	19	18	2	7	5	11	12	6	16	16
16	7	1	14	20	3	2	19	10	17	17	3	5	1	12	16	10	0	20	10	6
3	13	12	15	3	7	3	17	7	5	0	16	10	11	18	15	14	3	11	20	12
16	20	18	4	0	9	0	9	19	5	8	9	17	17	9	7	19	15	15	19	10
16	9	17	8	15	20	10	9	4	6	2	7	6	7	17	11	10	16	2	13	7
7	12	18	4	14	18	4	6	10	18	10	5	11	12	8	0	14	10	8	1	7
4	4	17	8	1	7	16	3	19	6	6	4	16	1	19	3	6	14	2	10	15
19	15	15	8	5	10	4	17	13	17	16	9	6	14	20	16	17	14	12	15	10
18	1	20	2	11	8	2	15	12	16	11	17	12	19	18	10	16	9	17	6	20
5	1	15	17	19	6	16	11	9	17	19	1	14	4	8	5	17	20	13	14	19
14	11	7	13	7	8	7	9	10	19	4	7	12	10	5	12	18	1	9	1	11
11	16	4	12	9	18	13	7	7	5	20	6	3	7	15	14	14	0	7	18	6
12	6	2	8	17	20	18	1	7	4	6	20	11	15	17	3	18	2	15	15	15
2	9	10	11	18	14	16	11	20	1	11	5	10	14	4	12	6	18	2	2	20
3	3	3	1	9	14	17	16	14	9	14	20	10	6	16	4	4	9	13	12	2
2	5	15	8	17	19	8	1	11	15	6	10	4	19	10	11	4	2	1	17	16
4	18	14	13	20	0	8	10	12	1	13	1	11	14	10	12	4	13	7	2	7

TABLE II. ELECTRIC FIELDS IN ALL POSITIONS

0,0	-17,0	-33,9	-37,5	-57,2	-60,6	-75,2	-63,8	-83,5	-63,3	-69,9	-82,5	-60,0	-93,1	-97,4	-114,2	-100,7	-105,6	-85,8	-111,2	-91,4
-17,0	-18,6	-20,5	-22,0	-23,1	-24,1	-24,8	-25,5	-26,1	-26,6	-27,0	-27,4	-27,8	-28,1	-28,5	-28,8	-29,0	-29,3	-29,5	-29,8	-30,0
-17,5	-20,5	-34,4	-22,6	-20,3	-24,3	-22,6	-25,6	-33,7	-26,6	-39,7	-27,5	-24,3	-28,2	-25,0	-28,8	-41,2	-29,3	-36,2	-29,8	-27,7
-33,9	-22,0	-22,6	-33,7	-24,0	-24,6	-32,9	-25,8	-26,3	-35,4	-27,2	-27,6	-48,5	-28,2	-28,5	-36,9	-29,1	-29,4	-36,5	-29,8	-30,0
-28,1	-23,1	-27,5	-24,0	-53,2	-25,1	-34,3	-26,1	-30,7	-26,9	-23,8	-27,7	-32,8	-28,3	-25,8	-28,9	-47,3	-29,4	-26,8	-29,9	-41,2
-37,5	-24,1	-24,3	-24,7	-25,1	-52,9	-25,9	-26,3	-26,7	-27,1	-34,5	-27,8	-28,1	-28,4	-28,7	-39,1	-29,2	-29,5	-29,7	-29,9	-52,8
-56,6	-24,8	-21,3	-40,6	-22,6	-25,9	-36,2	-26,6	-23,6	-44,5	-36,9	-28,0	-51,8	-28,5	-38,6	-33,8	-26,2	-29,5	-45,9	-30,0	-26,7
-40,7	-25,5	-25,6	-25,8	-26,1	-26,3	-26,6	-46,8	-27,3	-27,6	-27,9	-28,1	-28,4	-28,7	-46,3	-29,2	-29,4	-29,6	-29,8	-30,1	-30,3
-38,6	-26,1	-23,1	-26,3	-38,9	-26,7	-39,3	-27,3	-65,9	-27,8	-25,8	-28,3	-46,1	-28,8	-35,1	-29,3	-39,0	-29,7	-26,7	-30,1	-44,3
-50,4	-26,6	-26,6	-35,0	-26,9	-27,1	-28,2	-27,6	-27,8	-59,1	-28,3	-28,5	-24,3	-29,0	-29,2	-36,3	-29,6	-29,8	-44,3	-30,2	-30,4
-48,9	-27,0	-24,7	-27,2	-23,4	-66,8	-36,2	-27,9	-38,9	-28,3	-78,8	-28,7	-25,8	-29,1	-39,2	-43,9	-38,0	-29,9	-41,9	-30,3	-53,0
-41,3	-27,4	-27,5	-27,6	-27,7	-27,8	-28,0	-28,1	-28,3	-28,5	-28,7	-73,4	-29,1	-29,3	-29,5	-29,7	-29,9	-30,1	-30,2	-30,4	-30,6
-56,2	-27,8	-33,7	-39,4	-37,4	-28,1	-54,4	-28,4	-22,8	-39,1	-33,0	-29,1	-36,5	-29,5	-38,6	-24,4	-22,8	-30,2	-43,0	-30,5	-43,1
-68,1	-28,1	-28,2	-28,2	-28,3	-28,4	-28,5	-28,7	-28,8	-29,0	-29,1	-29,3	-29,5	-83,2	-29,8	-30,0	-30,1	-30,3	-30,5	-30,6	-30,8
-77,5	-28,5	-41,2	-28,5	-40,7	-28,7	-26,0	-76,3	-25,7	-29,2	-37,8	-29,5	-26,9	-29,8	-81,4	-30,1	-39,9	-30,4	-26,8	-30,7	-35,6
-83,9	-28,8	-28,8	-36,8	-28,9	-27,5	-24,4	-29,2	-29,3	-48,5	-22,0	-29,7	-49,8	-30,0	-30,1	-67,7	-30,4	-30,5	-39,3	-30,8	-35,8
-57,8	-29,0	-38,2	-29,1	-41,1	-29,2	-27,1	-29,4	-82,7	-29,6	-41,9	-29,9	-49,1	-30,1	-26,4	-30,4	-63,0	-30,7	-28,5	-30,9	-24,8
-84,5	-29,3	-29,3	-29,4	-29,4	-29,5	-29,5	-29,6	-29,7	-29,8	-29,9	-30,1	-30,2	-30,3	-30,4	-30,5	-30,7	-59,9	-30,9	-31,1	-31,2
-86,0	-29,5	-39,7	-54,4	-40,8	-29,7	-47,1	-29,8	-38,2	-61,0	-40,2	-30,2	-36,2	-30,5	-28,1	-47,3	-39,2	-30,9	-72,6	-31,2	-39,9
-58,5	-29,8	-29,8	-29,8	-29,9	-29,9	-30,0	-30,1	-30,1	-30,2	-30,3	-30,4	-30,5	-30,6	-30,7	-30,8	-30,9	-31,1	-31,2	-84,7	-31,4
-65,1	-30,0	-26,7	-30,0	-38,7	-57,2	-36,3	-30,3	-35,9	-30,4	-51,8	-30,6	-52,6	-30,8	-27,7	-45,8	-52,5	-31,2	-35,9	-31,4	-106,6